

**Cytometric
characteristics of
bacterioplankton
cells**

F. Van Wambeke et al.

Relationships between cytometric characteristics of high and low nucleic-acid bacterioplankton cells, bacterial production and environmental parameters along a longitudinal gradient across the Mediterranean Sea

F. Van Wambeke¹, P. Catala^{2,3}, and P. Lebaron^{2,3}

¹CNRS, Université de la Méditerranée, Laboratoire de Microbiologie, Géochimie et Ecologie Marines, UMR 6117, case 901, Campus de Luminy, 13 288 Marseille cedex 9, France

²UPMC Univ. Paris 06, Laboratoire ARAGO – Observatoire Océanologique, 66651 Banyuls/mer, France

³CNRS, UMR 7621, LOMIC, Observatoire Océanologique, 66651 Banyuls/mer, France

Title Page

Abstract

Introduction

Conclusions

References

Tables

Figures

⏪

⏩

◀

▶

Back

Close

Full Screen / Esc

Printer-friendly Version

Interactive Discussion



Received: 29 October 2010 – Accepted: 2 November 2010 – Published: 10 November 2010

Correspondence to: F. Van Wambeke (france.van-wambeke@univmed.fr)

Published by Copernicus Publications on behalf of the European Geosciences Union.

BGD

7, 8245–8279, 2010

**Cytometric
characteristics of
bacterioplankton
cells**

F. Van Wambeke et al.

Title Page

Abstract

Introduction

Conclusions

References

Tables

Figures



Back

Close

Full Screen / Esc

Printer-friendly Version

Interactive Discussion

Abstract

Heterotrophic bacterioplankton abundance and production were determined along vertical (down to bathypelagic layers) and latitudinal (from 4.9° E to 32.7° E) gradients across the Mediterranean Sea in early summer 2008. Abundance and flow cytometric characteristics (green fluorescence and side scatter signals) of high nucleic acid (HNA) and low nucleic acid (LNA) bacterial cells were investigated using flow cytometry. Contrarily to what is generally observed, the percentage of total bacteria represented by HNA cells (%HNA, range 30–69%) decreased with increased bacterial production (range 0.15–44 ng C l⁻¹ h⁻¹) although this negative relation was poorly explained (log-log regression $r^2 = 0.19$). The %HNA as well as the mean side scatter of this group increased significantly with depth in the meso and bathypelagic layers. Our results demonstrated that vertical stratification with regard to chlorophyll distribution above, within or below the deep chlorophyll maximum plays an important role in influencing the distribution of cells, and in the relationships between the flow cytometric parameters and environmental variables such as chlorophyll *a* or bacterial production. Relationships between green fluorescence and side scatter of both HNA and LNA cells depended largely on chlorophyll distribution over the water column, suggesting that the dynamic link between HNA and LNA cells differs vertically.

1 Introduction

Flow cytometry has been proven to be a powerful tool when studying microbial communities. In samples from aquatic environments, the bacterioplankton cells tend to cluster into at least 2 or 3 distinct fractions based on differences in the side scatter signal (SSC, related to the size, density and morphology of the cells) and in the relative green fluorescence (related to the nucleic acid content of the cells). These later fractions are more generally named HNA cells (cells with high nucleic acid content) and LNA cells (cells with low nucleic acid content, Lebaron et al., 2001). Many papers have reported

BGD

7, 8245–8279, 2010

Cytometric characteristics of bacterioplankton cells

F. Van Wambeke et al.

Title Page

Abstract

Introduction

Conclusions

References

Tables

Figures

◀

▶

◀

▶

Back

Close

Full Screen / Esc

Printer-friendly Version

Interactive Discussion

abundances of HNA and LNA cells over a wide range of environmental samples, from oligotrophic to eutrophic environments. SSC and green fluorescence information can be analysed and recorded at the same frequency as abundance, so providing a valuable data set on the bacterial communities whose role in terms of ecological significance, remains unclear. In addition, due to the difficulty in acquiring reproducible protocols (due to instrumental differences, storage conditions and the type of nucleic acid stain used), study inter-comparisons have generally been made on population abundance, and few have considered cytometric characteristics. Corzo et al. (2005) examined distributions through a 0–100 m water column in the Drake passage and Gerlache Straits during the austral summer. SSC and green fluorescence of HNA cells were closely related to chlorophyll *a* whereas those of LNA cells were not. In contrast, Sherr et al. (2006) used green fluorescence in relation to environmental ancillary parameters and showed that the ratios HNA/LNA for abundance and green fluorescence were remarkably stable along large inshore-offshore gradients in the northeast Pacific Ocean, concluding that HNA cells were not more responsive than LNA cells to chlorophyll variability. Bouvier et al. (2007) depicted these cytometric characteristics over a broad range of trophic conditions (bacterial production covering 4 orders of magnitude, from 0.01 to 11.6 $\mu\text{g C l}^{-1} \text{h}^{-1}$ and chlorophyll *a* 0.2 to 69 $\mu\text{g l}^{-1}$). These authors showed that these characteristics changed greatly in different ecosystems and along productivity gradients. The patterns they observed in cytometric parameters did not support the simple, dichotomous view of HNA and LNA bacteria as active and inactive cells, as hypothesized by early cell sorting experiments (Lebaron et al., 2001; Servais et al., 2003). The general conclusion from literature is that HNA bacteria are larger and more active on a cell basis than LNA bacteria. Overall, despite these advances, the contribution of LNA cells in total bacterial production is still a subject of much debate (Longnecker et al., 2006; Sherr et al., 2006; Scharek and Latasa, 2007; Moran et al., 2010).

The Mediterranean Sea is largely oligotrophic over much of the year, and has a wide gradient of oligotrophy from the West to the East. The BOUM (Biogeochemistry from

BGD

7, 8245–8279, 2010

Cytometric characteristics of bacterioplankton cells

F. Van Wambeke et al.

Title Page

Abstract

Introduction

Conclusions

References

Tables

Figures

⏪

⏩

◀

▶

Back

Close

Full Screen / Esc

Printer-friendly Version

Interactive Discussion

the Oligotrophic to the Ultra-oligotrophic Mediterranean) cruise carried out in early summer, June–July 2008, offered the opportunity to obtain bacterial abundance and production data over a large longitudinal and vertical gradient. A large number of samples were analysed using an unique procedure/instrument enabling us to investigate flow cytometric characteristics in relation to environmental properties along both vertical and horizontal gradients. The aim of this study was: (i) to explore the factors that determines the variability in abundances and cytometric properties of HNA and LNA cells in Mediterranean Sea waters, including the deep sea and (ii) to explore HNA-LNA cells connexions through relationships between cytometric parameters themselves. The strengths of relationships were examined according to the distribution of chlorophyll by dividing vertical layers.

2 Material and methods

2.1 Study area and sample collection

This work was carried out during the “BOUM” cruise on the *r/v Atalante* during June–July 2008. The cruise was planned as a transect of stations encompassing a large longitudinal gradient in the Mediterranean Sea (Fig. 1). Samples were collected using a rosette of 24×12 I Niskin bottles mounted on a CTD system. Total chlorophyll *a* (TChl-*a*) was analyzed using HPLC (Ras et al., 2008) and the data for vertical and horizontal profiles are presented in Moutin et al. (2010) and Crombet et al. (2010). The numbered stations represented the majority of the area were occupied briefly and sampled at different times of the day. All these numbered stations were investigated for bacterial abundance and only one over two for bacterial production (1, 3, 5, 7, 9, 11, 13, 15, 17, 19, 21, 24, 25). Sites designated by letters (A, B and C) were localized at the centre of anticyclonic gyres and each studied for 4 day periods. During this time, up to 4 depth profiles for bacterial abundance and production were sampled, three at 09:00 a.m., and one at 02:00 a.m. The whole data set was used to describe bacterial

BGD

7, 8245–8279, 2010

Cytometric characteristics of bacterioplankton cells

F. Van Wambeke et al.

Title Page

Abstract

Introduction

Conclusions

References

Tables

Figures

⏪

⏩

◀

▶

Back

Close

Full Screen / Esc

Printer-friendly Version

Interactive Discussion

abundance over 45 vertical profiles (498 data) while BP was studied over 25 profiles (198 data).

2.2 Flow cytometric analysis of bacteria

Aliquots of 1.8 ml were taken for heterotrophic bacterioplankton (sensus stricto referring to heterotrophic prokaryotes) were fixed with 2% (*w/v*) formaldehyde (PFA) solution, stored for at least 30 min at room temperature, frozen in liquid nitrogen and then stored at -80°C until samples could be processed on shore.

Samples were left to thaw at room temperature and stained with SYBR Green I (Invitrogen – Molecular Probes) at 0.025% (vol/vol) final concentration for 15 min at room temperature in the dark (Lebaron et al., 1998; Obernosterer et al., 2008). Counts were performed using the FacsCalibur flow cytometer (Becton Dickinson) equipped with an air-cooled argon laser (488 nm, 15 mW). The sheath fluid was filtered ($<0.2\ \mu\text{m}$) seawater. Stained bacterial cells, excited at 488 nm, were discriminated and enumerated according to their right-angle light scatter (SSC, related to cell size) and green fluorescence was measured at 530/30 nm. The speed of the analysis was dependant on the bacterial abundance of the sample, typically the volume analyzed was around $20\ \mu\text{l}$ (low speed). The subsequent cell concentration estimation was determined from the flow rate, which was calculated by weighing one tube of milliQ water before and after a 5 min run of the cytometer (this flow rate calibration was done after each five sample tubes). Fluorescent beads ($1.002\ \mu\text{m}$; Polysciences Europe) were systematically added to each sample as an internal standard and used to normalize values of single cell variables. Thus, the fluorescence and side scatter values of cells were standardized to those of the reference beads to account for potential differences in measurement conditions (all samples were analysed during a 6 month-period by the same analyst). In a plot of green fluorescence versus red fluorescence we were able to distinguish photosynthetic prokaryotes which were removed from non-photosynthetic prokaryotes. Bacteria with a high nucleic acid content (HNA cells) were discriminated from bacteria with a low nucleic acid content (LNA cells). Each subgroup was delimited

BGD

7, 8245–8279, 2010

Cytometric characteristics of bacterioplankton cells

F. Van Wambeke et al.

Title Page

Abstract

Introduction

Conclusions

References

Tables

Figures

◀

▶

◀

▶

Back

Close

Full Screen / Esc

Printer-friendly Version

Interactive Discussion



on the SSC versus green fluorescence plot by drawing a gate, and cell abundance was determined in each subgroup. The cytometric noise corresponded to particles which could not be assigned to any population, and this noise was sometimes close to the LNA subgroup.

2.3 Bacterial production

“Bacterial” production (BP – sensus stricto referring to heterotrophic prokaryotic production –) was determined by [³H] leucine incorporation applying the centrifugation method (Smith and Azam, 1992). Duplicate 1.5 mL samples were incubated with a mixture of [4,5-³H]leucine (Perkin Elmer, specific activity 115 Ci mmol⁻¹) and nonradioactive leucine at final concentrations of 16 and 7 nM, respectively for layers down to 200 m. Samples were incubated in the dark at the respective in situ temperatures for 2–5 h depending on the expected activity. We preliminarily checked that the incorporation of leucine was linear with time. Incubations were stopped by adding of trichloroacetic acid (TCA) to a final concentration of 5%. To facilitate the precipitation of proteins, bovine serum albumin (BSA, Sigma, 100 mg L⁻¹ final concentration) was added prior to centrifugation which was carried out at 16 000 g for 10 min. After discarding the supernatant, 1.5 ml of 5% TCA was added and the samples were vigorously shaken using a vortex then centrifuged again. A final centrifuge treatment was made with 80% ethanol. The radioactivity incorporated into the pellet was counted using a Packard LS 1600 Liquid Scintillation Counter. A factor of 1.5 kg C mol leucine⁻¹ was used to convert the incorporation of leucine to carbon equivalents, assuming no isotopic dilution. This was checked on 3 occasions with concentration kinetics (range of concentrations 3 to 50 nM, isotopic dilution between 1.01 and 1.07). Deeper samples, with a lower expected activity, were incubated in 50 ml tubes, with 10 nM final concentration of [4,5-³H]leucine. They were incubated in the dark at in situ temperature for 15–20 h, fixed with formalin (1% final concentration) and filtered through 0.2 μm Millipore GS/WP filters before TCA extraction (5% final) and a 80% ethanol rinse. Filters were dissolved in 1 ml of ethyl acetate before addition of Ultima Gold MV scintillation cocktail. Errors

Cytometric characteristics of bacterioplankton cells

F. Van Wambeke et al.

Title Page

Abstract

Introduction

Conclusions

References

Tables

Figures

⏪

⏩

◀

▶

Back

Close

Full Screen / Esc

Printer-friendly Version

Interactive Discussion



associated with the variability between replicate measurements (half the difference between the two replicates) averaged 6% and 8% for BP values determined using the centrifuge (surface samples) and filtration (deep samples) methods, respectively.

2.4 Statistical analysis and groups of data

5 Abundance variables and cytometric characteristics as well as ancillary environmental parameters (temperature, chlorophyll, BP) were \log_{10} transformed in order to achieve normality and homogeneity of variances. Model II regressions were used to examine relationships between 2 parameters, as both are subjected to variability. Model I was used to examine the relationship with temperature or depth. Note that the coefficient
10 of determination is the same whatever the model used.

Relationships were examined following 4 different groups of samples:

- “surface” samples located between the surface and the dcm layer,
- “dcm” samples at the dcm,
- “below dcm” corresponds to samples taken between the dcm and 250 m,
- 15 – “deep” corresponds to samples taken below 250 m.

3 Results

3.1 Distribution and variability of biological and physico-chemical parameters

The stations were located between 43.2° N, 4.93° E (Rhone river Mouth) and 33.7° N, 32.7° E (South of Cyprus, on the sea mount Erathostène, Fig. 1). All stations were
20 situated in the continental slope or open Sea (except at the Sicily Strait: stations 14, 382 m and 17, 116 m and at the Rhone river Mouth: station 27, 105 m), with bottom depths reaching up to 3321 m (station 12). There was a classical west east gradient

BGD

7, 8245–8279, 2010

Cytometric characteristics of bacterioplankton cells

F. Van Wambeke et al.

Title Page

Abstract

Introduction

Conclusions

References

Tables

Figures

⏪

⏩

◀

▶

Back

Close

Full Screen / Esc

Printer-friendly Version

Interactive Discussion



in terms of the deepening of the deep chlorophyll maximum layer, which varied from 50 m at station 25 (with $1.7 \mu\text{g } T\text{Chl-}a \text{ l}^{-1}$) to 125 m at station 9 ($0.22 \mu\text{g } T\text{Chl-}a \text{ l}^{-1}$, Fig. 2). Surface temperature (5 m) reached a maximum of 27.5°C (station 12 in the Levantine Sea) with lowest temperatures at station 27 (17.2°C , Rhone river Mouth) and decreasing with depth down to 13.3°C in the Eastern Basin and 12.8°C in the Western Basin (Fig. 4).

3.2 Total abundance and production

Total bacterial abundance ranged from 0.15 to $13.4 \times 10^5 \text{ ml}^{-1}$ (Table 1). Abundance decreased from West to East and with depth, but the distribution patterns along the surface layers were highly variable (Fig. 2). The coefficient of variation for total abundance was lower than that of total chlorophyll *a* (*TChl-a*) or bacterial production (BP) for a given layer. For example, in the “surface” layers, i.e. above the dcm, the coefficient of variation for total abundance was 33% ($n = 192$) whereas those of *TChl-a* and BP were 74% and 60%, respectively (Table 1).

BP ranged from $0.1 \text{ ng C l}^{-1} \text{ h}^{-1}$ (650 m, station C) to $43.9 \text{ ng C l}^{-1} \text{ h}^{-1}$ (Sicily Strait, 5 m, station 15), and $41 \text{ ng C l}^{-1} \text{ h}^{-1}$ at the station closest to the Rhône river plume (25 m, station 25, Fig. 2). Based on integrated *TChl-a* (concentrations measured down to 250 m), the most oligotrophic station was station 8, with $16.1 \text{ mg } T\text{Chl-}a \text{ m}^{-2}$ whereas the richest was station 25 ($55.3 \text{ mg } T\text{Chl-}a \text{ m}^{-2}$).

Relationships between bacterial biomass (BB) and bacterial production were calculated assuming 12 fgC per cell (Fig. 3). Model I was used in addition to model II in order to compare our slopes with those recorded in the literature. The relationship is greater ($r^2 = 0.7$) when all the data are pooled due to the large range of BP and BB data including, meso and bathypelagic layers. Indeed, the r^2 determination coefficients are much lower when considering the different layers “surface”, “dcm” or “below dcm” ($r^2 = 0.24$ to 0.54) (Table 2). The regression slope calculated using model I is also higher when the whole data set is considered.

Cytometric characteristics of bacterioplankton cells

F. Van Wambeke et al.

Title Page

Abstract

Introduction

Conclusions

References

Tables

Figures

⏪

⏩

◀

▶

Back

Close

Full Screen / Esc

Printer-friendly Version

Interactive Discussion



The slopes obtained (0.32–0.36) for “dcm” and “below dcm” layers, respectively, are due to a weak bottom up control of bacterial biomass based on Billen et al. (1990) and Ducklow (1992); whereas the slope of 0.27 ($r^2 = 0.24$) obtained within subsurface layers would indicate a low bottom-up control. However such differences are less obvious when interpreting the slopes derived from the model II regression (0.44 to 0.57, Table 2).

TChl-a explained poorly variability in BP (29%). There was little or no relationship between *TChl-a* and BP for “surface” layers, although relationships were stronger for the “dcm” and “below dcm” categories ($r^2 = 0.52$ and 0.53, Table 2).

3.3 HNA and LNA abundance

All samples had two HNA and LNA cell fractions discernable by fluorescence versus SSC cytograms. HNA cell abundances ranged from 7.7×10^3 to 6.1×10^5 ml⁻¹, and those of LNA cells from 6.5×10^3 to 7.3×10^5 ml⁻¹ (Fig. 4). Box plot distributions of HNA and LNA cell abundances relating to layer (“surface”, “dcm”, “below dcm”, “deep”) were similar (Fig. 5a, b). Firstly, there was a greater variability within the “surface” and “dcm” categories. Secondly neither HNA nor LNA cell abundances were statistically different in the “surface” when compared to the “dcm” layers (ANOVA, threshold chosen at $p = 0.01$), but significantly decreased “below the dcm” and in the “deep” layers (ANOVA, $p < 0.01$). The decrease in HNA and LNA cell abundances with depth (log-log regressions abundance-depth) were significant for “dcm”, “below dcm” and “deep” layers (r^2 ranged 0.33–0.66, for all regressions $p < 0.01$). Depth could not explain the variability in abundance in the “surface” layers ($r^2 = 0.03$ and 0.02 for LNA and HNA cell abundances, respectively, Fig. 4). Finally depth could explain the variability in the percentage of HNA cell abundance (%HNA) in the “deep” layers (log-log regression, $r^2 = 0.59$, $n = 53$), whereas for the other layers the correlation was insignificant.

Bacterial production was responsible for 65% and 70% of the variability in HNA and LNA cell abundance, respectively (Table 3), but the positive slope of the log-log regression was significantly higher for the LNA cells (0.52 ± 0.02 versus 0.43 ± 0.02

Cytometric characteristics of bacterioplankton cells

F. Van Wambeke et al.

[Title Page](#)[Abstract](#)[Introduction](#)[Conclusions](#)[References](#)[Tables](#)[Figures](#)[⏪](#)[⏩](#)[◀](#)[▶](#)[Back](#)[Close](#)[Full Screen / Esc](#)[Printer-friendly Version](#)[Interactive Discussion](#)

with model I, 0.62 versus 0.53, with model II, data not shown). Consequently, %HNA decreased slightly with increasing BP (the log-log regression was barely significant, $r^2 = 0.19$, $n = 198$, Table 3, Fig. 6d). However, the log-log relation between %HNA and BP was insignificant for “surface”, “below dcm” and “deep” layers, and BP explained (with a positive slope) only 21% of the variability of % HNA in the “dcm” layers (Table 3).

TChl-a also explained a large variability in HNA and LNA cell abundances. Both log-log distributions of HNA and LNA cell abundances showed a significant, positive slope following *TChl-a* concentrations (slopes model II: 0.31, $r^2 = 0.59$; 0.34, $r^2 = 0.60$, respectively, Table 3). These slopes were significant for all data sets, but also within the 3 chlorophyll layers when considered independently (“surface”, “dcm” and “above dcm”). However data from surface layers exhibited a greater dispersion, resulting in less significant determination coefficients (Table 3, data not shown).

3.4 Patterns in cytometric parameters in relation to depth, chlorophyll and bacterial production

Standardized SSC of HNA and LNA cells ranged from 0.0093 to 0.0265 and from 0.078 to 0.0185, respectively. Standardized green fluorescence of HNA and LNA cells ranged from 0.18 to 0.44 and from 0.050 to 0.097, respectively (Figs. 4, 6 and 7). The coefficient of variation of SSC was slightly higher for HNA cells (21%) than for LNA cells (17%). This was the same for green fluorescence (15% versus 12%). While green fluorescence characteristics were very distinct between the HNA and LNA cells whatever the depth (Fig. 4i, j), SSC differences were slight within surface layers but higher in meso and bathy pelagic layers (Figs. 4g, h, 5c, d).

SSC decreased with depth in “surface” layers (log-log regressions, model I, $p < 0.001$, $r^2 = 0.37$ for HNA cells $p < 0.001$, $r^2 = 0.46$ for LNA cells, data Fig. 4g) and increased in “deep” layers ($p < 0.001$, $r^2 = 0.66$ for HNA cells, $p < 0.001$, $r^2 = 0.27$ for LNA cells, data Fig. 4h). This was more pronounced for HNA cells. Indeed, SSC of this group increased 6 times more rapidly with depth than the SSC of the LNA cells (Fig. 4h).

BGD

7, 8245–8279, 2010

Cytometric characteristics of bacterioplankton cells

F. Van Wambeke et al.

Title Page

Abstract

Introduction

Conclusions

References

Tables

Figures

⏪

⏩

◀

▶

Back

Close

Full Screen / Esc

Printer-friendly Version

Interactive Discussion



Cytometric characteristics of bacterioplankton cells

F. Van Wambeke et al.

Title Page

Abstract

Introduction

Conclusions

References

Tables

Figures

◀

▶

◀

▶

Back

Close

Full Screen / Esc

Printer-friendly Version

Interactive Discussion



Green fluorescence of LNA cells decreased slightly with depth and thus, depth poorly explained the variations in green fluorescence of LNA cells (log-log regressions, $r^2 = 0.24$, $n = 493$, data Figs. 4 and 5e). In contrast, the green fluorescence of the HNA cells increased significantly with depth ($r^2 = 0.51$, Figs. 4i, j, 5f).

The SSC of HNA and LNA cells exhibited a significant decrease with *TChl-a* within “surface” layers ($r^2 = 0.45$ and 0.49 respectively, Table 3). On the contrary, this trend was low, inexistent or even slightly reversed for “dcm” or “below dcm” layers. Relationships between SSC and BP were insignificant or slightly positive for the LNA cells and insignificant or slightly negative for the HNA cells (Table 3, Fig. 6b).

While relationships between SSC of the HNA cells and *TChl-a* were more noticeable within “surface” layers, those between green fluorescence of the HNA cells and *TChl-a* were noticeable mainly below the dcm (negative relationship, $r^2 = 0.44$, Table 3). Green fluorescence of the HNA cells decreased with increasing BP ($r^2 = 0.44$), this being more marked for layers “below dcm”. Contrary to this, green fluorescence of the LNA cells increased slightly with BP, this increase being particularly obvious in the “surface” and “dcm” layers (Table 3, Fig. 6a).

HNA/LNA ratios of both SSC and green fluorescence decreased with increasing bacterial production ($r^2 = 0.34$ and 0.58 , respectively), although this decrease was more noticeable for fluorescence (slope model II = -0.16) than for SSC (slope model II = -0.09 , data Fig. 6c). The decrease in the HNA/LNA ratio was significant for SSC within “below dcm” layers ($r^2 = 0.29$, slope -0.09) while the decrease in the HNA/LNA ratio for green fluorescence was more regular whatever chlorophyll layer was considered (Fig. 6c).

3.5 Relationships between cytometric parameters

The ANOVA analysis of SSC and green fluorescence based on the “chlorophyll” layers suggests that this discrimination criterion was particularly appropriate in explaining the variability in green fluorescence of HNA cells ($n = 489$, $F = 356$), and to a lesser degree of LNA cells ($F = 32$). This discrimination criterion was more or less equal to explain

variability in SSC of the two groups ($F = 90$ for LNA cells, $F = 76$ for HNA cells, Fig. 4c, d, e, f).

There was a positive and highly significant relationship between the SSC of HNA and LNA cells, which was particularly marked for “surface” layers (slope model II 0.96, $r^2 = 0.84$, $n = 192$ Fig. 7b). This trend, although still significant, decreased for other layers showing lower slopes and r^2 : slope 0.68, $r^2 = 0.43$, $n = 45$ for “dcm”; slope 0.65, $r^2 = 0.13$, $n = 201$ for “below dcm”; and then slope 0.43 ± 0.04 , $r^2 = 0.44$, $n = 55$ for “deep” layers.

Any relationships between the green fluorescence of HNA and LNA cells, showed relatively weaker coefficients of determination ($r^2 = 0.29$ for surface layers, 0.23 for dcm layers) or were insignificant at $p = 0.01$ for layers below dcm ($p = 0.8$) and deep layers ($p = 0.05$). Consequently, the cytometric characteristics of the HNA and LNA cells are not independent from each other, but the relationships seem to follow distinct patterns relative to chlorophyll vertical distribution.

The relationships between green fluorescence and SSC of the HNA cells exhibited different patterns depending on the layer considered. The slope was weakly negative but significant above dcm ($r^2 = 0.08$), the relation was insignificant at dcm at $p = 0.01$, and finally the slope was weakly positive, and then strongly positive below the dcm and in the deeper layers ($r^2 = 0.22$ and, $r^2 = 0.62$, respectively). Relationships between green fluorescence and SSC for LNA cells were insignificant whatever the layer at $p = 0.01$, except for a slightly positive correlation for “surface” layers ($r^2 = 0.18$).

4 Discussion

The rationale to base our data analysis on different water column layers characterised by different patterns of chl concentrations (“surface”, “dcm” and “below dcm”) is inspired from a number of previous studies that have shown strong vertical structure of phytoplankton groups and nutrient distribution according the position of the dcm. Bacterial communities below and above the dcm probably exhibit different taxonomic structures

BGD

7, 8245–8279, 2010

Cytometric characteristics of bacterioplankton cells

F. Van Wambeke et al.

Title Page

Abstract

Introduction

Conclusions

References

Tables

Figures

⏪

⏩

◀

▶

Back

Close

Full Screen / Esc

Printer-friendly Version

Interactive Discussion



which to some extent is related to the phytoplankton vertical distribution (Ghiglione et al., 2008) as well as to differing limiting factors: labile carbon below DCM, and mostly nutrient limitation within surface layers (Sala et al., 2002; Van Wambeke et al., 2002; Tanaka et al., 2010; Talarmin et al., 2010). The “surface” layers were exposed to large temperature gradients during our study (21.5–27.5 °C within 5m down to 13.5–17.5 °C at the dcm), as well as large ranges of incident light, creating additional sources for variability in the superimposition of vertical and longitudinal trends. The “dcm” layer represented an ideal ecological boundary in our study which enabled data to be compared from stations distributed along longitudinal gradients, where the transparency of water, depth of nutriclines and dcm varied greatly (Pujo Pay et al., 2010; Crombet et al., 2010).

Relationships described between BP, LNA and HNA cell abundances and cytometric parameters, and environmental variables tracking resource indices (BP, *T*Chl-*a*), or physical gradients (temperature, depth) or relationships between the cytometric parameters themselves were clearly chlorophyll layer – specific. Indeed, some relations were insignificant for pooled data but are significant within a specific layer. Both slopes and determination coefficients changed within the different layers, as well as the sign of the slope (Fig. 7c, Table 3). These results confirm the previous comments of Bouvier et al. (2007) which demonstrated ecosystem-specific relationships within the cytometric structure, but in this work we clearly demonstrate that the notion of ecosystem specificity can be divided again, here based on chlorophyll distribution through the water column.

4.1 Deep layers

In contrast to the work of Bouvier et al. (2007) we examined relationships within the cytometric parameters of HNA and LNA cells not only for surface layers, but throughout the water column. Variability with depth may be important since environmental parameters like abundance, chlorophyll and/or temperature, as well as the productivity gradient (reflected by BP) also varied with depth. The most striking feature was the

BGD

7, 8245–8279, 2010

Cytometric characteristics of bacterioplankton cells

F. Van Wambeke et al.

Title Page

Abstract

Introduction

Conclusions

References

Tables

Figures

⏪

⏩

◀

▶

Back

Close

Full Screen / Esc

Printer-friendly Version

Interactive Discussion



4.2 LNA HNA Abundance, percentage of HNA relationships with environmental parameters

The percentage of HNA cells relative to total abundance (%HNA) varies greatly within different environments (11–85%, see Bouvier et al., 2007, including data from salt marshes to open marine systems). It can vary seasonally at a fixed station over a large range (30–84% within specific surface layers 0–20 m in northern Spain coastal waters, Moran and Calvo-Diaz, 2009). In our study %HNA exhibited a narrower range (30–69%). %HNA decreased slightly, but significantly, with BP and showed a very weak negative correlation with chlorophyll (log-log regressions, Table 3).

Some investigators have suggested that HNA and LNA cells represent active and less active (or inactive) components. Therefore, the %HNA was generally studied in relation to variables tracking the productivity index of the system, like chlorophyll concentration or bacterial production (Corzo et al., 2005, Moran et al., 2007). On large scale productivity gradients, the correlation between % HNA and chlorophyll is generally positive (Bouvier et al., 2007; Chl-*a* gradient 0.1 to 69 $\mu\text{g l}^{-1}$, Sherr et al., 2006; Chl-*a* gradient 0.2 to 20 $\mu\text{g l}^{-1}$). Over smaller chlorophyll gradients, diverse results have been reported. Moran and Calvo Diaz (2009) studying the yearly temporal evolution at a coastal temperate marine station, obtained a chlorophyll gradient of 0–4 $\mu\text{g l}^{-1}$ within subsurface layers and showed a positive correlation. In contrast, and based on a seasonal study of a lake where Chl *a* ranged from 0.1 to 11 $\mu\text{g l}^{-1}$, Nishimura et al. (2005) obtained a negative correlation. Finally, Corzo et al. (2005) in the Drake Passage and along the Antarctic coast, found no correlation over a chlorophyll gradient ranging from 0.05 to 5 $\mu\text{g l}^{-1}$.

Using our data set, including a weak chlorophyll gradients varying between limits of detection and 1.7 $\mu\text{g l}^{-1}$ (Table 1), the correlation was negative, but *TChl-a* explained slightly variability of %HNA ($r^2 = 0.07$, Table 3). However, both HNA and LNA cell abundances were significantly correlated with *TChl-a* in our study and this relation was valid along the different sub-groups of chlorophyll categories. For instance in

BGD

7, 8245–8279, 2010

Cytometric characteristics of bacterioplankton cells

F. Van Wambeke et al.

Title Page

Abstract

Introduction

Conclusions

References

Tables

Figures

⏪

⏩

◀

▶

Back

Close

Full Screen / Esc

Printer-friendly Version

Interactive Discussion

examining only the “dcm” layer (there is only one dcm layer per station) whose depth is largely depended on the west-east gradient and the mesoscale structures (Moutin et al., 2010; Pujo Pay et al., 2010), the correlation was significant within this layer (Table 3). The slope of the regression of abundance versus chlorophyll was slightly higher for HNA than for LNA cells within the “dcm” layer, suggesting that the HNA cells were very responsive to changes in phytoplankton stocks in the “dcm” layer. For other layers (“surface”, “below dcm”), the responsiveness of both groups was very close and thus, they were responding equally to *TChl-a* variations in terms of abundance. Sherr et al. (2006) noticed also that both groups responded similarly with regard to phytoplankton biomass. The same trend was observed for bacterial production (Table 3), with higher slopes for the regression abundance = $f(\text{BP})$ within “dcm” layers for HNA groups. At this layer, the %HNA was also significantly and positively correlated with BP ($r^2 = 0.21$).

4.3 Green fluorescence and SSC relationships with environmental parameters

Very few studies have explored cytometric properties like green fluorescence or SSC with environmental variables. HNA cells are considered as a very active and dynamic with high specific activities (Servais et al., 1999; Lebaron et al., 2001; Longnecker et al., 2005, 2006; Talarmin et al., 2010). It was shown that within the HNA cells, BP increased with SSC and fluorescence signals (Lebaron et al., 2002). Since the green fluorescence is related to the apparent nucleic acid content per cell, we could hypothesise that the more the green fluorescence of a group varies, the more this group is adapted to respond to environmental parameters. As seen in the literature, this seems to be the case for the HNA cells. For instance exploring winter waters in the Antarctic between 0 and 100 m, Corzo et al. (2005) found that variability in chlorophyll did not explain the green fluorescence of LNA cells but rather that of HNA cells. These authors also found that chlorophyll gave more variability in the SSC of HNA cells (47%) than the SSC of LNA cells (5%). In our study, we found a negative correlation between green fluorescence and chlorophyll on one hand, and green fluorescence and BP on

BGD

7, 8245–8279, 2010

Cytometric characteristics of bacterioplankton cells

F. Van Wambeke et al.

Title Page

Abstract

Introduction

Conclusions

References

Tables

Figures

⏪

⏩

◀

▶

Back

Close

Full Screen / Esc

Printer-friendly Version

Interactive Discussion



the other hand, only at selected layers, mainly “below dcm” for the HNA cells and “surface” and “dcm” for LNA cells (Table 3).

If the high variability of green fluorescence is a factor reflecting better adaptation to changes in environmental factors like BP or chlorophyll, then the HNA cells appear to be better adapted to “below dcm” layers and LNA to “surface” and “dcm” layers (Table 3). This is in agreement with the work of Talarmin et al. (2010) which show, through ³H leucine labelling coupled to cell sorting, that the contribution of LNA to the bulk leucine incorporation rates is higher in “surface” waters, than at the “dcm” and “below dcm” layers. The comparison with other studies in which chlorophyll peaked within surface layers and where nutrients are not limiting, like in Antarctic waters (Corzo et al., 2005), is particularly difficult. The fact that both fluorescence and SSC signals of HNA cells respond negatively to BP and *TChl-a* at layers “below dcm”, where both the latter parameters decrease, suggests that the switch from nutrients to carbon limitation might influence positively the richness in nucleic acids of the HNA cells as a physiological response to different starvation factors. Another (not exclusive) explanation could be a drastic change in the taxonomic composition of the HNA cells facing new limiting factors and carbon source in this layer, in relation to stratification of nutrients and phytoplankton populations (Ghiglione et al., 2008; Van Wambeke et al., 2009).

On the contrary, the variation of cytometric parameters, with regard to environmental factors, seemed more important for LNA cells within “surface” and “dcm” layers. At these layers, BP and chlorophyll explained roughly 22–29% in the variability of the green fluorescence of LNA cells. Sharek and Latasa (2007) observed larger SSC (on both LNA and HNA cells) in surface waters of NW Mediterranean Sea, which was attributed to coastal and/or Rhone river plume influence. However, such explanation is unlikely in our samples which are from the open sea. Within surface layers, however, a drastic gradient of temperature is present (from 26 to 15 °C which explains the high variability of SSC in both groups ($r^2 = 0.41$ for HNA and 0.45 for LNA, positive relation between SSC and temperature, results not shown). In addition, in the oligotrophic, stratified conditions prevailing in our study, *TChl-a* does not reflect the distribution of

BGD

7, 8245–8279, 2010

Cytometric characteristics of bacterioplankton cells

F. Van Wambeke et al.

Title Page

Abstract

Introduction

Conclusions

References

Tables

Figures

⏪

⏩

◀

▶

Back

Close

Full Screen / Esc

Printer-friendly Version

Interactive Discussion

phytoplankton biomass through the water column due to photoadaptation. It is also possible that some source of the variability, especially for surface layers, could be due to daily variability of cytometric parameters as all profiles were not sampled at the same time of the day.

5 4.4 HNA/LNA relationships

The overall relationship for green fluorescence between the two groups was almost non-existent (Fig. 7a, $r^2 = 0.016$) and stronger for SSC (Fig. 7b, $r^2 = 0.54$), but still weaker than in Bouvier et al. (2007). Thus, the concept of co-variation of cytometric characteristics of LNA and HNA cells depicted over large productivity gradients by these authors was not clearly demonstrated here. However, the strong relationship between the SSC of HNA and LNA cells obtained in “surface” layers (Fig. 7b, $r^2 = 0.84$) suggests that some cellular characteristics, such as membrane structure, taxonomy, and/or any aspect of cell physiology that influence SSC, is varying to a larger degree within this layer and that SSC for both groups is influenced by the ecosystem structure in this layer.

Although the pattern of green fluorescence – SSC relationships of the HNA group is insignificant overall, the links between these two variables is apparent in “deep” layers ($r^2 = 0.62$, Fig. 6c). The patterns of change in taxonomic structure and effect of pressure could be direct causes of such links between cytometric parameters within the HNA cells. Indeed, as described above, the HNA cells had a greater contribution in terms of abundance in the meso and bathypelagic zones.

5 Conclusions

This study is the first to investigate the cytometric properties of HNA and LNA cells over both vertical and longitudinal scales in the oligotrophic Mediterranean Sea. Although the proportions of the HNA and LNA cells did not vary over large percentages, their

BGD

7, 8245–8279, 2010

Cytometric characteristics of bacterioplankton cells

F. Van Wambeke et al.

Title Page

Abstract

Introduction

Conclusions

References

Tables

Figures

⏪

⏩

◀

▶

Back

Close

Full Screen / Esc

Printer-friendly Version

Interactive Discussion



cytometric characteristics showed distinct properties and relationships between themselves and between other environmental variables. The covariation between green fluorescence and side scatter of both groups depended largely on chlorophyll distribution over the water column, suggesting that the dynamic link between HNA and LNA cells is different vertically according light, temperature, taxonomic composition and/or that of the other components of the microbial food web, to which they are strongly coupled through delivery of DOM/regenerated nutrients (resource control). Combination of new emergent tools such as cell sorting coupled to activity measurements, cloning/sequencing analysis of sorted groups (Guillebault et al., 2010), and investigation of individual cell composition with emergent techniques (Twining et al., 2008) will be essential to our understanding of the ecological meaning of the ubiquitous presence of LNA and HNA cells and their connections.

Acknowledgements. This research was funded by the French INSU-CNRS & by the SESAME project (Southern European Seas: Assessing and Modelling Ecosystem Changes), EC Contract No GOCE-036949, funded by the European Commission's Sixth Framework Programme. The authors would like to thank Thierry Moutin for leadership of the project and chief scientist of the BOUM cruise, Stella Psarra and Joséphine Ras for total chlorophyll sampling and analysis, Claude Courties and Christian Tamburini for helpful discussions.



The publication of this article is financed by CNRS-INSU.

BGD

7, 8245–8279, 2010

Cytometric characteristics of bacterioplankton cells

F. Van Wambeke et al.

Title Page

Abstract

Introduction

Conclusions

References

Tables

Figures

⏪

⏩

◀

▶

Back

Close

Full Screen / Esc

Printer-friendly Version

Interactive Discussion



References

- Al Ali, B., Garel, M., Cuny, P., Miquel, J.-C., Toubal, T., Robert, A., and Tamburini, C.: Luminous bacteria in the deep-sea waters near the ANTARES underwater neutrino telescope (Mediterranean Sea), *Chem. Ecol.*, 26, 57–72, 2010.
- 5 Bouvier, T., Del Giorgio, P., and Gasol, J.: A comparative study of the cytometric characteristics of high and low nucleic acid bacteriaoplankton cells from different aquatic ecosystems, *Environ. Microbiol.*, 9, 2050–2066, 2007.
- Bouvier, T., Troussellier, M., Anzil, A., Courties, C., and Servais, P.: Using light scatter signal to estimate biovolume by flow cytometry, *Cytometry*, 44, 188–194, 2001.
- 10 Corzo, A., Rodríguez-Gálvez, S., Lubian, L., Sobrino, C., Sangrá, P., and Martínez, A.: Antarctic marine bacterioplankton subpopulations discriminated by their apparent content of nucleic acids differ in their response to ecological factors, *Polar Biol.*, 29, 27–39, 2005.
- Crombet, Y., Leblanc, K., Quéguiner, B., Moutin, T., Rimmelin, P., Ras, J., Claustre, H., Leblond, N., Oriol, L., and Pujo-Pay, M.: Deep silicon maxima in the stratified oligotrophic Mediterranean Sea, *Biogeosciences Discuss.*, 7, 6789–6846, doi:10.5194/bgd-7-6789-2010, 2010.
- 15 Felip, M., Andreatta, S., Sommaruga, R., Straskrabova, V., and Catalan, J.: Suitability of flow cytometry for estimating bacterial biovolume in natural plankton samples: comparison with microscopy data, *Appl. Environ. Microbiol.*, 73, 4508–4514, 2007.
- Gasol, J. M., Alonso-Saez, L., Vaqué, D., Baltar, F., Calleja, M., Duarte, C. M., and Aristegui, J.: Mesopelagic prokaryoteic bulk and single cell heterotrophic activity and community composition in the NW Africa – Canary Islands coastal-transition zone, *Prog. Oceanogr.*, 83, 189–196, 2009.
- 20 Ghiglione, J. F., Palacios, C., Marty, J. C., Mével, G., Labrune, C., Conan, P., Pujo-Pay, M., Garcia, N., and Goutx, M.: Role of environmental factors for the vertical distribution (0–1000 m) of marine bacterial communities in the NW Mediterranean Sea, *Biogeosciences*, 5, 1751–1764, doi:10.5194/bg-5-1751-2008, 2008.
- 25 Guillebault, D., Laghdass, M., Catala, P., Obernosterer, I., and Lebaron, P.: Enhanced environmental diversity revealed by an improved method of bacterial cell capture and 16S rRNA gene amplification after flow cytometry cell sorting, *Appl. Environ. Microbiol. Methods*, 76, 7352–7355, 2010.
- 30 Jochem, F. J.: Morphology and DNA content of bacterioplankton in the northern gulf of Mexico: analysis by epifluorescence microscopy and flow cytometry, *Aquat. Microb.Ecol.*, 25, 179–

Cytometric characteristics of bacterioplankton cells

F. Van Wambeke et al.

Title Page

Abstract

Introduction

Conclusions

References

Tables

Figures

◀

▶

◀

▶

Back

Close

Full Screen / Esc

Printer-friendly Version

Interactive Discussion



194, 2001.

La Ferla, R., Giudice, A., and Maimone, G.: Morphology and LPS content for the estimation of marine bacterioplankton biomass in the Ionian Sea, *Scientia Marina*, 68, 23–31, 2004.

Lebaron, P., Servais, P., Agogu e, H., Courties, C., and Joux, F.: Does the High Nucleic Acid Content of Individual Bacterial Cells Allow Us To Discriminate between Active Cells and Inactive Cells in Aquatic Systems?, *Appl. Environ. Microbiol.*, 67, 1775–1782, 2001.

Lebaron, P., Servais, P., Baudoux, A.-C., Bourrain, M., Courties, C., and Parthuisot, N.: Variations of bacterial-specific activity with cell size and nucleic acid content assessed by flow cytometry, *Aquat. Microb. Ecol.*, 28, 131–140, 2002.

Longnecker, K., Sherr, B. F., and Sherr, E. B.: Activity and phylogenetic diversity of bacterial cells with high and low nucleic acid content and electron transport system activity in an upwelling ecosystem, *Appl. Environ. Microbiol.*, 71, 7737–7749, 2005.

Longnecker, K., Sherr, B. F., and Sherr, E. B.: Variation in cell specific rates of leucine and thymidine incorporation by marine bacteria with high and low nucleic acid content off the Oregon coast, *Aquat. Microb. Ecol.*, 43, 113–125, 2006.

Mary, I., Heywood, J. L., Fuchs, B., Amann, R., Tarran, G., Burkhill, P., and Zubkov, M.: SAR11 dominance among metabolically active low nucleic acid bacterioplankton in surface waters along an Atlantic meridional transect, *Aquat. Microb. Ecol.*, 45, 107–113, 2006.

Moran, X. A. and Calvo-Diaz, A.: Single cell vs bulk activity properties of coastal bacterioplankton over an annual cycle in a temperate ecosystem, *FEMS Microb. Ecol.*, 67, 43–56, 2009.

Moran, X. A., Bode, A., Suarez, L. A., and Nogueira, E.: Assessing the relevance of nucleic acid content as an indicator of marine bacterial activity, *Aquat. Microb. Ecol.*, 46, 141–152, 2007.

Moutin, T., Van Wambeke, F., and Prieur, L.: Introduction to the Biogeochemistry from the Oligotrophic to the Ultraoligotrophic Mediterranean experiment: the BOUM program, in preparation, 2010.

Pujo-Pay, M., Conan, P., Oriol, L., Cornet-Barthaux, V., Falco, C., Ghiglione, J.-F., Goyet, C., Moutin, T., and Prieur, L.: Integrated survey of elemental stoichiometry (C, N, P) from the Western to Eastern Mediterranean Sea, *Biogeosciences Discuss.*, 7, 7315–7358, doi:10.5194/bgd-7-7315-2010, 2010.

Nishimura, Y., Kim, C., and Nagata, T.: Vertical and seasonal variations of bacterioplankton subgroups with different nucleic acid contents: possible regulation by phosphorus, *Appl.*

BGD

7, 8245–8279, 2010

Cytometric characteristics of bacterioplankton cells

F. Van Wambeke et al.

Title Page

Abstract

Introduction

Conclusions

References

Tables

Figures

⏪

⏩

◀

▶

Back

Close

Full Screen / Esc

Printer-friendly Version

Interactive Discussion

subpopulations in seawater based on SYTO 13 staining of nucleic acids, *FEMS Microbiol. Ecol.*, 29, 319–330, 1999.

Twining, B. S., Baines, S., Vogt, S., and de Jonge, M. D.: Exploring ocean biogeochemistry by single cell microprobe analysis of protist elemental composition, *J. Eukaryot. Microbiol.*, 55, 151–162, 2008.

Van Wambeke, F., Christaki, U., Giannakourou, A., Moutin, T., and Souvemerzoglou, K.: Longitudinal and vertical trends of bacterial limitation by phosphorus and carbon in the Mediterranean Sea, *Microb. Ecol.*, 43, 119–133, 2002.

Van Wambeke, F., Ghiglione, J.-F., Nedoma, J., Mével, G., and Raimbault, P.: Bottom up effects on bacterioplankton growth and composition during summer-autumn transition in the open NW Mediterranean Sea, *Biogeosciences*, 6, 705–720, doi:10.5194/bg-6-705-2009, 2009.

Zubkov, M., Fuchs, B., Tarran, G., Burkhill, P., and Amann, R.: Mesoscale distribution of dominant bacterioplankton groups in the North Sea in early summer, *Aquat. Microb. Ecol.*, 29, 135–144, 2002.

BGD

7, 8245–8279, 2010

Cytometric characteristics of bacterioplankton cells

F. Van Wambeke et al.

Title Page

Abstract

Introduction

Conclusions

References

Tables

Figures

⏪

⏩

◀

▶

Back

Close

Full Screen / Esc

Printer-friendly Version

Interactive Discussion

Cytometric characteristics of bacterioplankton cells

F. Van Wambeke et al.

Table 1. Ranges of Temperature, Salinity, Total chlorophyll *a* (*TChl-a*), Soluble Reactive Phosphorus (SRP), Total bacterial abundance (total ab), and bacterial production (BP) for the data set used for comparison of abundance and cytometric characteristics of HNA & LNA cells. Means, coefficient of variation and number of data for each group of water column partition: layers above the deep chlorophyll maximum (surface), layers at the deep chlorophyll maximum (“dcm”), layers below the dcm but above or equal to 250 m (“below dcm”), and layers below 250 m “deep”. bdl: below detection limits.

	Salinity (PSU)	temperature (pot, °C)	<i>TChl-a</i> (µg l ⁻¹)	SRP (µM)	total ab (×10 ⁵ ml ⁻¹)	BP (ng C l ⁻¹ h ⁻¹)
N	498	498	296	409	498	198
min	37.24	12.9	0.0004	bdl	0.15	0.15
max	39.65	27.5	1.7	0.393	13.40	43.9
mean	38.47	16.7	0.11	0.083	3.32	11.2
sd	0.58	3.5	0.16	0.114	2.05	9.5
surface	38.33 (1.8%, <i>n</i> = 192)	19.7 (18%, <i>n</i> = 192)	0.098 (74%, <i>n</i> = 111)	0.009 (159%, <i>n</i> = 109)	4.62 (33%, <i>n</i> = 192)	15.0 (60%, <i>n</i> = 110)
dcm	38.42 (1.6%, <i>n</i> = 45)	15.7 (7%, <i>n</i> = 45)	0.44 (67%, <i>n</i> = 30)	0.015 (117%, <i>n</i> = 29)	5.18 (43%, <i>n</i> = 45)	15.2 (61%, <i>n</i> = 24)
below dcm	38.63 (1.2%, <i>n</i> = 201)	14.9 (8%, <i>n</i> = 201)	0.059 (135%, <i>n</i> = 154)	0.112 (91%, <i>n</i> = 148)	2.25 (49%, <i>n</i> = 201)	3.62 (96%, <i>n</i> = 54)
deep	38.63 (0.4%, <i>n</i> = 55)	13.4 (5%, <i>n</i> = 55)		0.278 (36%, <i>n</i> = 53)	0.53 (110%, <i>n</i> = 55)	0.42 (123%, <i>n</i> = 10)

Title Page

Abstract Introduction

Conclusions References

Tables Figures

⏪ ⏩

◀ ▶

Back Close

Full Screen / Esc

Printer-friendly Version

Interactive Discussion



Cytometric characteristics of bacterioplankton cells

F. Van Wambeke et al.

Table 2. Model I and II linear regression analysis of (i) the relationships between log bacterial biomass ($\mu\text{g l}^{-1}$) and log bacterial production ($\mu\text{g C l}^{-1} \text{h}^{-1}$) and (ii) the relationships between log bacterial production ($\text{ng C l}^{-1} \text{h}^{-1}$) and *TChl-a* ($\mu\text{g l}^{-1}$). Determination coefficient (r^2), number of data (n), standard error (se).

		n	Model II slope	Model I slope \pm se	r^2
Log BB= f (log BP)	all data	198	0.572	+ 0.479 \pm 0.022	0.70
	surface	110	0.550	+ 0.273 \pm 0.046	0.246
	dcm	24	0.447	+ 0.329 \pm 0.064	0.543
	below dcm	54	0.525	+ 0.361 \pm 0.053	0.473
	deep	10	ns		ns
Log BP= f (log <i>TChl-a</i>)	all data	105	0.824	+ 0.449 \pm 0.068	0.297
	surface	59	ns		ns
	dcm	16	1.023	+ 0.741 \pm 0.188	0.525
	below dcm	30	0.509	+ 0.371 \pm 0.066	0.533

Title Page

Abstract

Introduction

Conclusions

References

Tables

Figures

◀

▶

◀

▶

Back

Close

Full Screen / Esc

Printer-friendly Version

Interactive Discussion

Cytometric characteristics of bacterioplankton cells

F. Van Wambeke et al.

[Title Page](#)
[Abstract](#)
[Introduction](#)
[Conclusions](#)
[References](#)
[Tables](#)
[Figures](#)
[Back](#)
[Close](#)
[Full Screen / Esc](#)
[Printer-friendly Version](#)
[Interactive Discussion](#)

Table 3. Relationships between flow cytometric parameters of HNA and LNA cells (abundance, SSC, green fluorescence) and %HNA versus *TChl-a* and versus BP. Data were log-log transformed before fitting with linear regressions. n : number of data, r^2 : determination coefficient, nd: not determined, ns: not significant (Significant threshold set at $p = 0.05$). For clarity, sign of slopes for weak correlations ($r^2 < 0.1$) were not indicated.

		relation with <i>TChl-a</i>			relation with BP		
		n	Sign of slope	r^2	n	sign of slope	r^2
HNA abundance	all data	296	+	0.59	198	+	0.65
	surface	111	+	0.32	110	+	0.25
	dcm	31	+	0.41	24	+	0.52
	below dcm	154	+	0.55	54	+	0.42
	deep			nd	10		ns
LNA abundance	all data	296	+	0.60	198	+	0.70
	surface	111	+	0.26	110	+	0.20
	dcm	31	+	0.40	24	+	0.49
	below dcm	154	+	0.64	54	+	0.46
	deep			nd	10		ns
% HNA	all data	296		0.07	198	–	0.19
	surface	111		ns	110		ns
	dcm	31	+	0.117	24	+	0.21
	below dcm	154		0.02	54		ns
	deep			nd	10		ns
SSC HNA	all data	296		ns	198		ns
	surface	111	–	0.45	110		ns
	dcm	31		ns	24		ns
	below dcm	154	–	0.14	54	–	0.12
	deep			nd	10		ns

Cytometric characteristics of bacterioplankton cells

F. Van Wambeke et al.

[Title Page](#)[Abstract](#)[Introduction](#)[Conclusions](#)[References](#)[Tables](#)[Figures](#)[⏪](#)[⏩](#)[◀](#)[▶](#)[Back](#)[Close](#)[Full Screen / Esc](#)[Printer-friendly Version](#)[Interactive Discussion](#)**Table 3.** Continued.

		relation with <i>TChl-a</i>			relation with BP		
		<i>n</i>	Sign of slope	<i>r</i> ²	<i>n</i>	sign of slope	<i>r</i> ²
SSC LNA	all data	296		0.03	198	+	0.11
	surface	111	–	0.49	110		ns
	dcm	31		ns	24	+	0.18
	below dcm	154		0.02	54		ns
	deep			nd	10		ns
fluo HNA	all data	296	–	0.37	198	–	0.44
	surface	111		ns	110		0.07
	dcm	31		ns	24		ns
	below dcm	154	–	0.44	54	–	0.29
	deep			nd	10		ns
fluo LNA	all data	296		0.01	198	+	0.232
	surface	111	–	0.22	110	+	0.23
	dcm	31	+	0.23	24	+	0.29
	below dcm	154		ns	54		ns
	deep			nd	10		ns

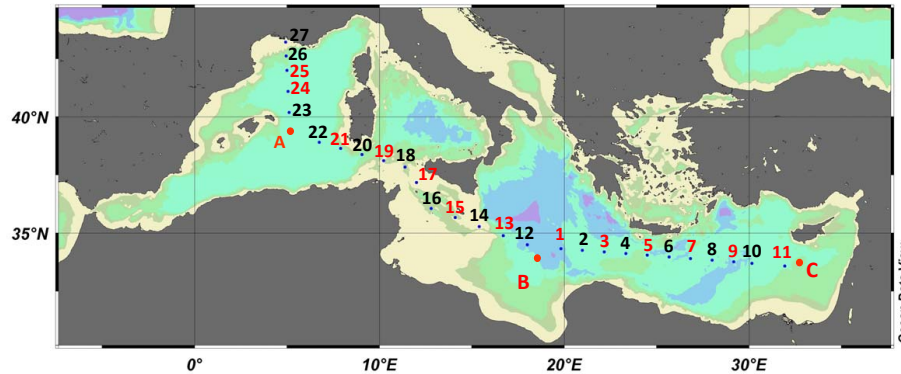


Fig. 1. Map of the BOUM transect. All stations were sampled for bacterial abundances and *TChl-a* whereas only stations indicated with a code in red were sampled for bacterial production.

BGD

7, 8245–8279, 2010

Cytometric characteristics of bacterioplankton cells

F. Van Wambeke et al.

Title Page

Abstract

Introduction

Conclusions

References

Tables

Figures

⏪

⏩

◀

▶

Back

Close

Full Screen / Esc

Printer-friendly Version

Interactive Discussion



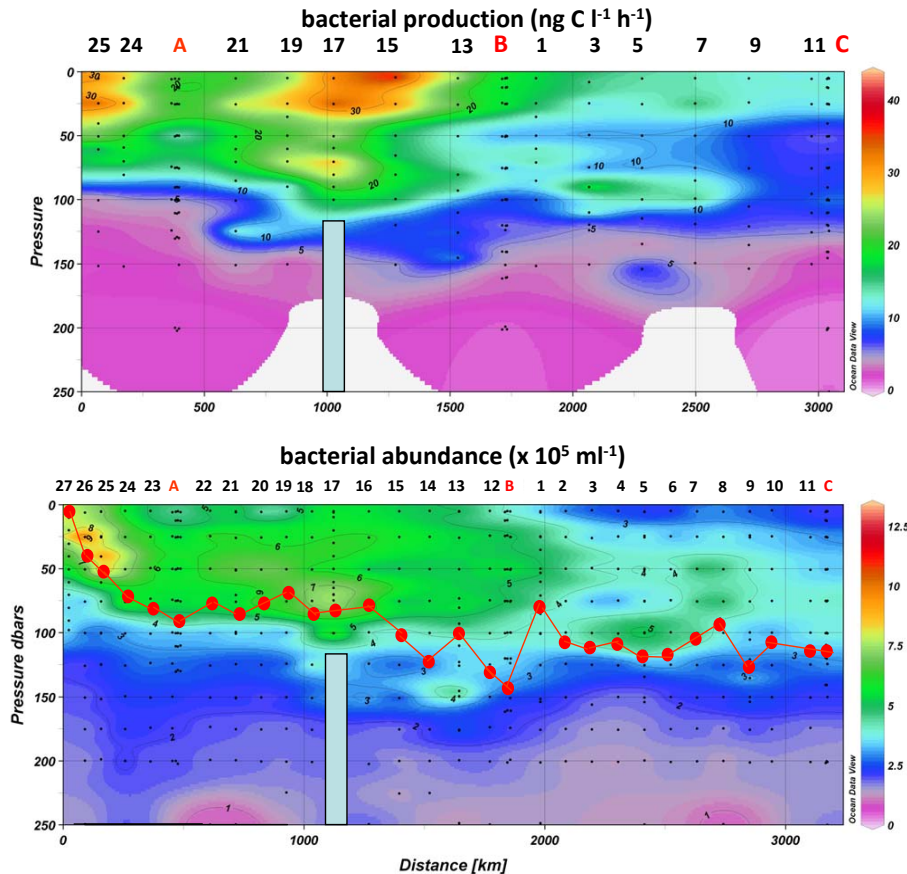


Fig. 2. Contour plot of total bacterial abundance and bacterial production along the BOUM transect, from the most north-western station (left) to the most eastern station (right) and for the 0–250 m layer. Depth of the deep chlorophyll maximum is also indicated (red dots).

Cytometric characteristics of bacterioplankton cells

F. Van Wambeke et al.

Title Page

Abstract

Introduction

Conclusions

References

Tables

Figures

⏪

⏩

◀

▶

Back

Close

Full Screen / Esc

Printer-friendly Version

Interactive Discussion

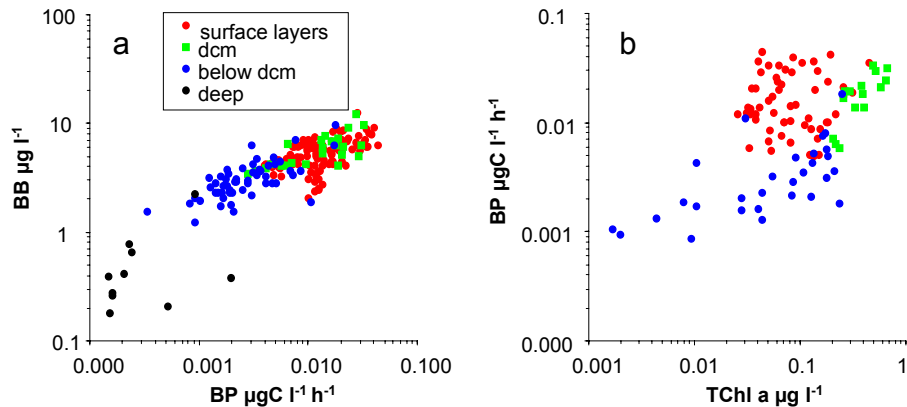


Fig. 3. (a) log log (base 10) representations of bacterial biomass versus bacterial production and bacterial production versus total chlorophyll *a*. the results of model I and II regressions are indicated in Table 2.

Cytometric characteristics of bacterioplankton cells

F. Van Wambeke et al.

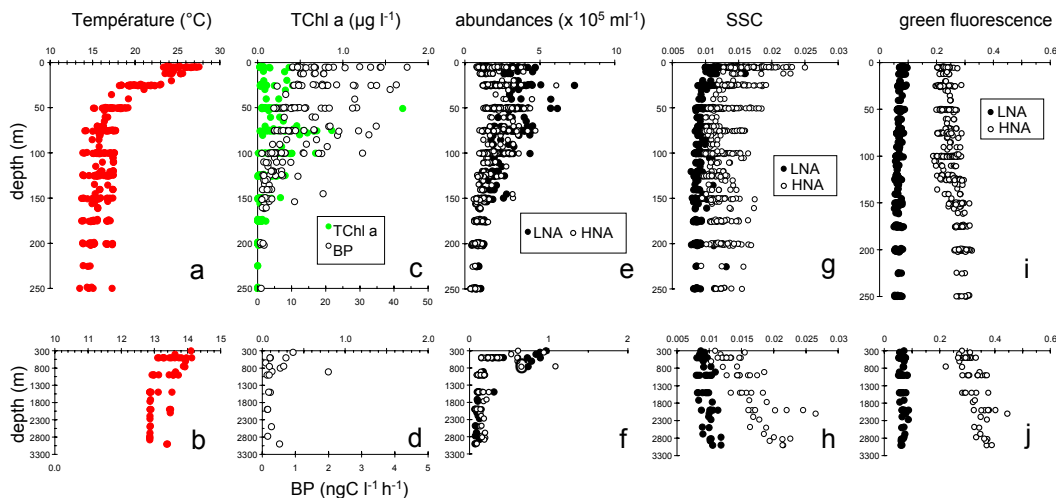


Fig. 4. Vertical distributions of temperature, total chlorophyll *a*, bacterial production, HNA and LNA abundances, side scatter signal (SSC) and green fluorescence signal. Note different scales for the deeper layers (bottom figures **b** and **f**).

Title Page

Abstract

Introduction

Conclusions

References

Tables

Figures

◀

▶

◀

▶

Back

Close

Full Screen / Esc

Printer-friendly Version

Interactive Discussion

Cytometric characteristics of bacterioplankton cells

F. Van Wambeke et al.

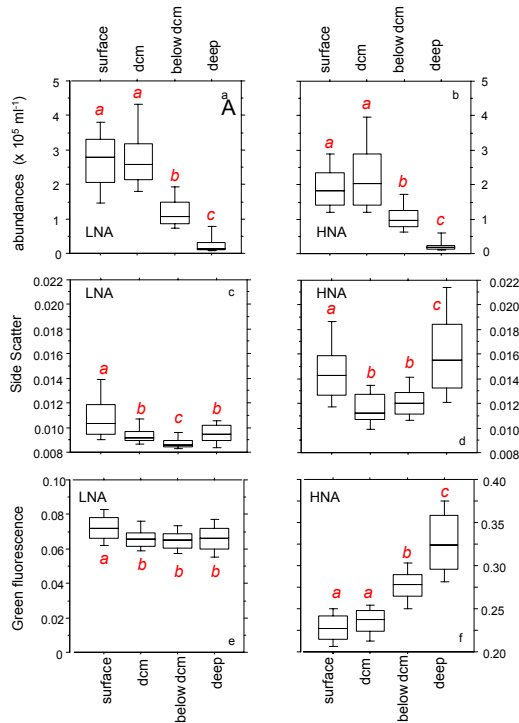


Fig. 5. Box plots showing distribution of abundance (**a**, **b**), green fluorescence (**c**, **d**) and side scatter (**e**, **f**) of subgroups LNA and HNA based on *TChl-a* distribution and depth along the water column layers above the deep chlorophyll maximum (“surface”), layers at the deep chlorophyll maximum (“dcm”), layers below the dcm but above or equal to 250 m (“below dcm”), and layers below 250 m (“deep”). Groups connected by the same letter (in italics & in red) are not significantly different at the 0.01 probability level (ANOVA & Fischer PLSD test on log-transformed data). Lower to the upper values are indicated, respectively, 10%, 25%, 50% (median), 75 and 90 % percentiles.

Cytometric characteristics of bacterioplankton cells

F. Van Wambeke et al.

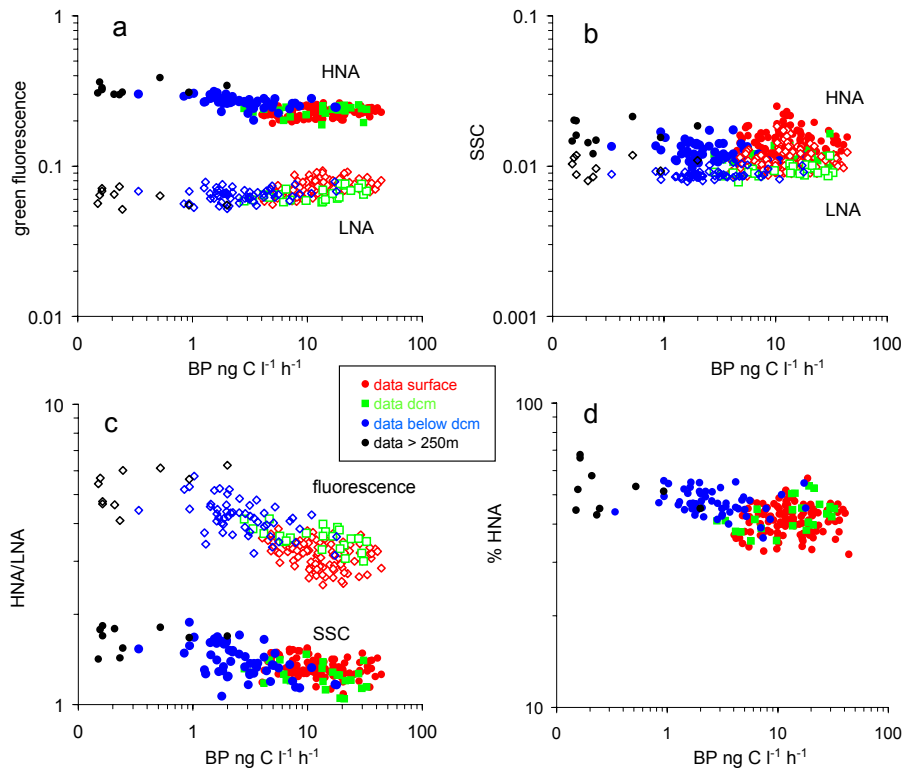


Fig. 6. Relationships between bacterial production and (a) the green fluorescence of HNA and LNA cells, (b) the Side Scatter of HNA and LNA cells, (c) the ratio of green fluorescence between HNA and LNA cells and the ratio of Side Scatter between HNA and LNA cells, (d) the percentage of HNA cells.

Title Page

Abstract Introduction

Conclusions References

Tables Figures

◀ ▶

◀ ▶

Back Close

Full Screen / Esc

Printer-friendly Version

Interactive Discussion

Cytometric characteristics of bacterioplankton cells

F. Van Wambeke et al.

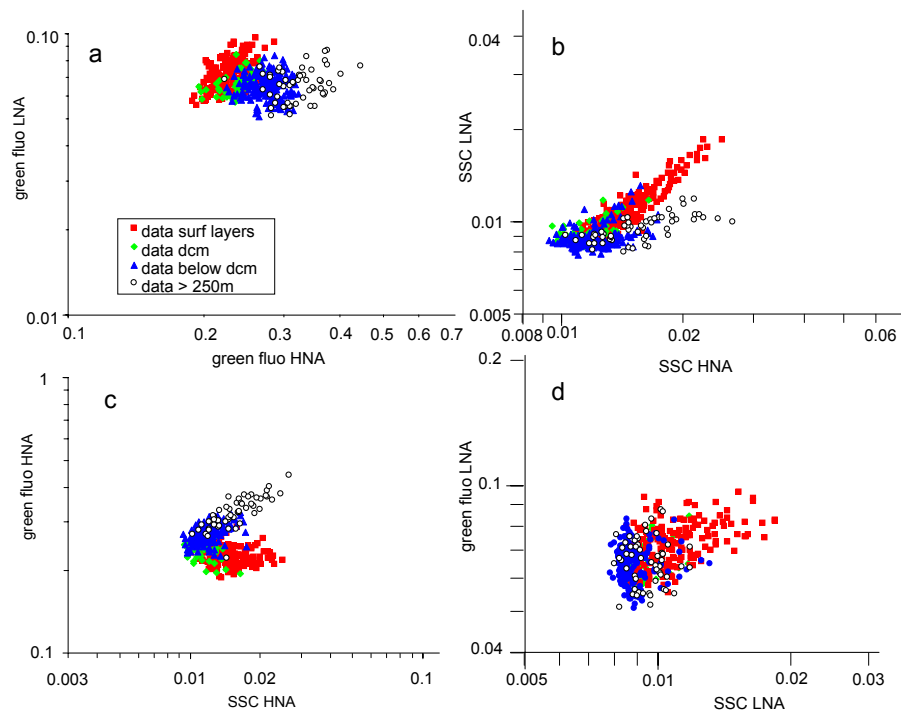


Fig. 7. Relationships between **(a)** HNA green fluorescence and LNA green fluorescence, **(b)** HNA side scatter and LNA side scatter, **(c)** green fluorescence and side scatter of HNA cells, **(d)** green fluorescence and side scatter of LNA cells **(d)**.

Title Page

Abstract

Introduction

Conclusions

References

Tables

Figures

◀

▶

◀

▶

Back

Close

Full Screen / Esc

Printer-friendly Version

Interactive Discussion